Genetic and biophysical basis of sudden unexplained nocturnal death syndrome (SUNDS), a disease allelic to Brugada syndrome

Matteo Vatta[1], Robert Dumaine[4], George Varghese[1], Todd A. Richard[4], Wataru Shimizu[5], Naohiko Aihara[5], Koonlawee Nademanee[6], Ramon Brugada[2], Josep Brugada[7], Gumpanart Veerakul[9], Hua Li[1], Neil E. Bowles[1], Pedro Brugada[8], Charles Antzelevitch[4] and Jeffrey A. Towbin[1,3,*]

[1]Department of Pediatrics (Cardiology), [2]Department of Medicine (Cardiology) and [3]Department of Molecular and Human Genetics, Baylor College of Medicine, Houston, TX, USA, [4]Masonic Medical Research Laboratory, Utica, NY, USA, [5]Department of Internal Medicine (Cardiology), National Cardiovascular Center, Osaka, Japan, [6]Department of Medicine (Cardiology), University of Southern California, Los Angeles, CA, USA, [7]Cardiovascular Institute, Hospital Clinic, University of Barcelona, Spain, [8]Cardiovascular Center, OLV Hospital, Aalst, Belgium and [9]Department of Cardiology, Bhumibol Adulyadej Hospital, RTAF, Bangkok, Thailand

Sudden unexplained nocturnal death syndrome (SUNDS), a disorder found in southeast Asia, is characterized by an abnormal electrocardiogram with ST-segment elevation in leads V1–V3 and sudden death due to ventricular fibrillation, identical to that seen in Brugada syndrome. We screened patients with SUNDS for mutations in *SCN5A*, the gene known to cause Brugada syndrome, as well as genes encoding ion channels associated with the long-QT syndrome. Ten families were enrolled, and screened for mutations using single-strand DNA conformation polymorphism analysis, denaturing high-performance liquid chromatography and DNA sequencing. Mutations were identified in *SCN5A* in three families. One mutation, R367H, lies in the first P segment of the pore-lining region between the DIS5 and DIS6 transmembrane segments of SCN5A. A second mutation, A735V, lies in the first transmembrane segment of domain II (DIIS1) close to the first extracellular loop between DIIS1 and DIIS2, whereas the third mutation, R1192Q, lies in domain III. Analysis of these mutations in *Xenopus* oocytes showed that the R367H mutant channel did not express any current and the likely effect of this mutation is to depress peak current due to the loss of one functional allele. The A735V mutant expressed currents with steady state activation voltage shifted to more positive potentials. The R1192Q mutation accelerated the inactivation of the sodium channel current. Both mutations resulted in reduced sodium channel current (I_{Na}) at a time corresponding to the end of phase 1 of the action potential, as described previously in the Brugada syndrome. Based upon these observations we suggest that SUNDS and Brugada syndrome are phenotypically, genetically and functionally the same disorder.

INTRODUCTION

Sudden unexplained nocturnal death syndrome (SUNDS) is a disorder found in southeast Asia, particularly Thailand, Japan, Philippines and Cambodia, which causes sudden cardiac death (usually in males) during sleep (1–3). This disorder, which is the most common cause of 'natural' death in the young, healthy Asian population, is called by many descriptive terms in the various countries, including pokkuri ('sudden unexplained death at night') in Japan, lai-tai ('died during sleep') in Thailand, and bangungut ('moaning and dying during sleep') in the Philippines.

The clinical features of SUNDS include ST-segment elevation in the right precordial leads (V1–V3), inconsistently

associated with right bundle branch block (RBBB) (Fig. 1) (2,3) and ventricular tachycardia and fibrillation (VF) on surface electrocardiogram (ECG). These clinical characteristics are similar to those of the Brugada syndrome, a disorder diagnosed in individuals of European descent (4–6).

The genetic cause of the Brugada syndrome was initially described by our group and shown to be due to mutations in the cardiac sodium channel gene, *SCN5A*. This has now been confirmed by others (7,8). In previous publications, we and others demonstrated that mutant sodium channels have a reduced sodium channel current (I_{Na}) due to rapid inactivation of the current or failure of the channel to express currents (9,10). Due to the apparent clinical similarities between
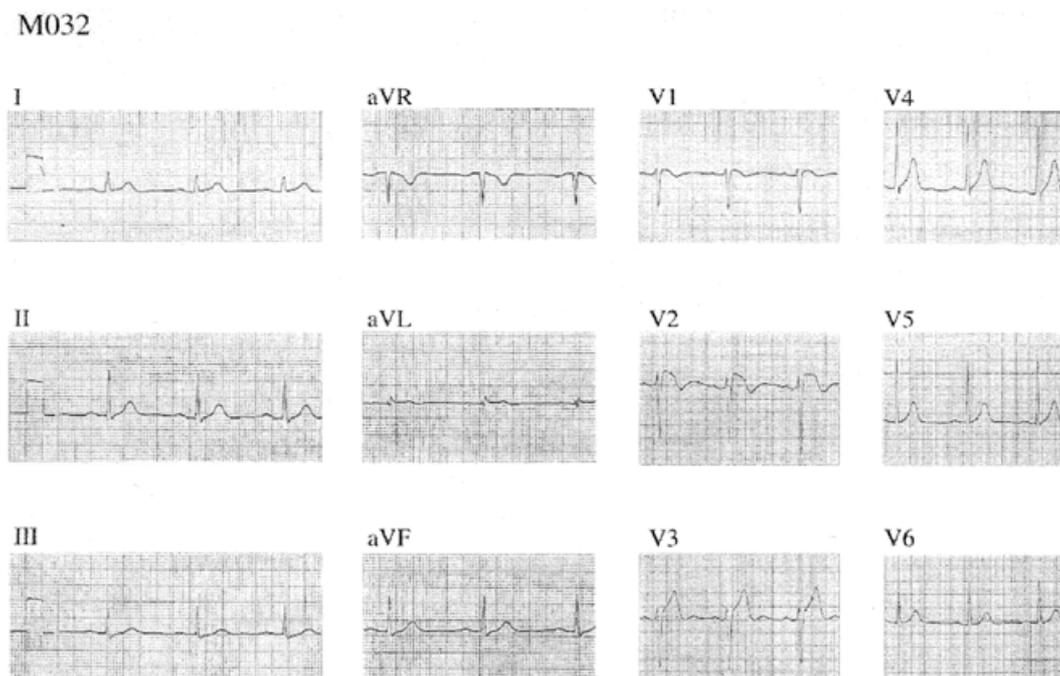
M032

Figure 1. ECG of SUNDS. Note the ST-segment elevation in leads V1–V3 in the proband of family M032, identical to the findings in Brugada syndrome.

Brugada syndrome and SUNDS, we speculated that these could be allelic disorders (or even the same disease). In this report, we describe the molecular analysis of patients with SUNDS and identify mutations in *SCN5A*, confirming this disorder to be genotypically, phenotypically and functionally identical to Brugada syndrome.

RESULTS

Mutation analysis

Ten probands with clinical evidence of SUNDS were screened for mutations in *KVLQT1* (11), *HERG* (11), *SCN5A* (9,11), *minK* (12) and *MiRP1* (13) using single-strand DNA conformation polymorphism (SSCP) analysis, denaturing high-performance liquid chromatography (DHPLC) and DNA sequencing. In three patients (M030, M032, M033), *SCN5A* mutations were identified. No mutations were identified in any of the other genes screened. Patient M030 is a sporadic case, whereas the other two cases were probands of families. One of these was a family with multiple affected individuals (family M032), and apparent autosomal dominant inheritance. The second family (M033) included a pair of affected Japanese dizygotic twins. One twin died unexpectedly during sleep at 4 months of age. The other twin had frequent VF episodes at 6 months of age and has been discussed previously (14). This living child and other family members were studied.

Patient M030. An abnormal conformer was identified in exon 9 of *SCN5A* in this sporadic case (Fig. 2A) and confirmed by DHPLC analysis (Fig. 2C). DNA sequence analysis revealed a G→A base substitution (G1100A) in exon 9 (Fig. 2B) leading to the substitution of an arginine by a histidine at codon 367 (R367H), which lies in the first P segment belonging to the
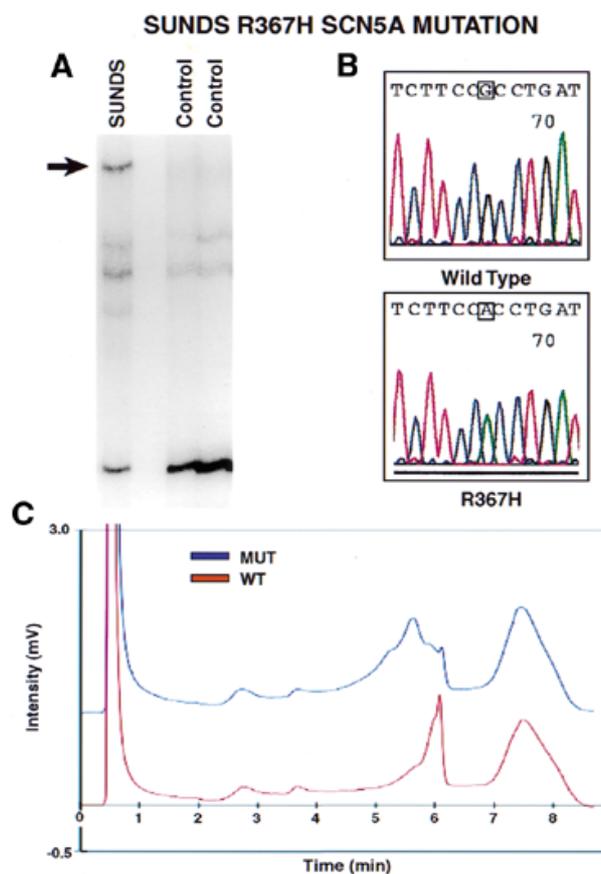
Figure 2. Mutation detection in sporadic case M030. (**A**) SSCP analysis demonstrates an abnormal conformer in the affected individual. (**B**) DNA sequence analysis identifies a G→A substitution in exon 9 of *SCN5A*, resulting in an amino acid substitution of arginine to histidine at codon 367 (R367H). (**C**) DHPLC confirms an abnormal migration pattern in the affected individual.
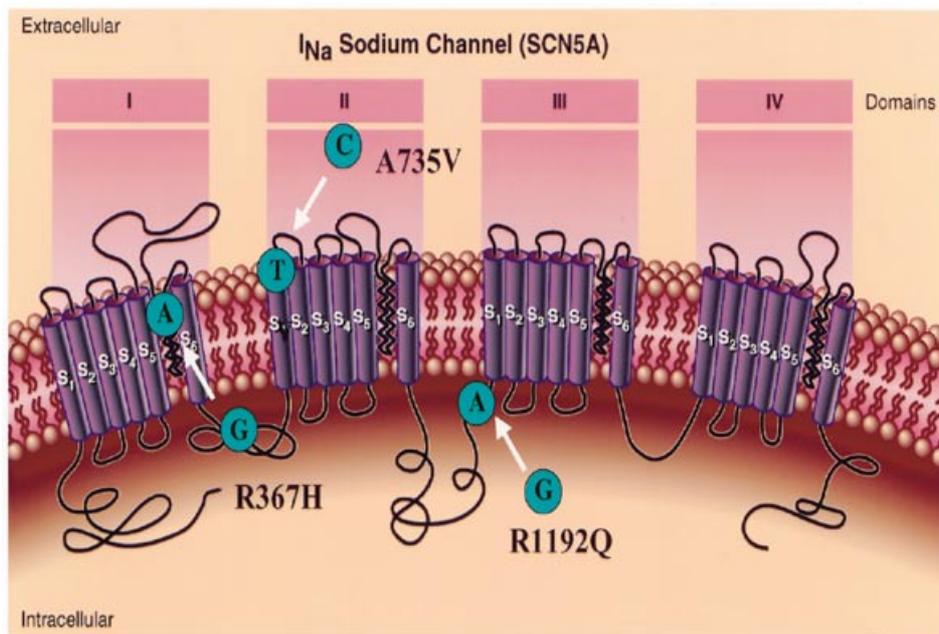
Figure 3. Illustration of the SUNDS mutations within the cardiac sodium channel *SCN5A*, as well as the locations of mutations previously identified in Brugada syndrome and LQTS patients.

pore-lining region between the DIS5 and DIS6 transmembrane segments of the cardiac sodium channel (Fig. 3). The P segment is a conserved region within the Na^+-channel family (15). This mutation was not found in other family members (including the parents) nor in 100 control individuals (200 chromosomes) of Asian descent (data not shown).

Family M032. A point mutation was identified in the proband of family M032. SSCP (Fig. 4A) and DHPLC analysis (Fig. 4C) identified an abnormality in exon 14, due to a C→T substitution (C2204T) (Fig. 4B) leading to a substitution of alanine by valine at codon 735 (A735V). This mutation lies in the first transmembrane segment of domain II (DIIS1) at the border with the first extracellular loop between DIIS1 and DIIS2 (Fig. 3). Screening of other family members identified the same mutation in the father and the son of the proband, both of whom had ECG abnormalities consistent with SUNDS. The unaffected family members and 100 control patients did not carry this mutation.

Family M033. A point mutation was identified in the proband of family M033, the surviving dizygotic twin. DHPLC analysis (Fig. 5A) identified an abnormality in exon 20, due to a G→A substitution (G3575A) (Fig. 5B) leading to a substitution of arginine by glutamine at codon 1192 (R1192Q). This mutation lies in the intracellular loop connecting the DIIS6 to DIIIS1 (Fig. 3). Screening of other family members identified the same mutation in the affected family members (data not shown). The unaffected family members and 100 control patients did not carry this mutation.

Biophysical analysis

To study the mechanism by which these mutations may contribute to the syndrome, heterologous expression in

Xenopus oocytes was performed. The mutant channel R367H did not express any current and the likely effect of this mutation is to depress I_{Na} due to the loss of one functional allele (Fig. 6A and C).

In contrast, expression of the A735V mutant appeared normal (Fig. 6B). Although visual inspection of the current traces suggested faster decay of A735V current, statistical analysis of the current decay fit to the sum of two exponential failed to show a significant increase of inactivation kinetics (Z-test for mean or ANOVA). However, the time to peak of the maximum current was significantly briefer for A735V (1.8 ± 0.1 ms) versus wild-type (WT) (2.2 ± 0.1 ms) (Fig. 7). The average maximum current was measured at –10 and –5 mV for WT and A735V, respectively. The shorter time to peak and shift of the voltage of maximum current for A735V was due to a 7 mV shift of the steady state activation curve towards more positive potentials (Fig. 7B).

Figure 8 shows that the shift in steady state activation leads to a significant reduction in A735V current at a time (3 ms) and over a range of potentials (–30 to 0 mV) corresponding to phase 1 of the epicardial right ventricular action potential.

The R1192Q mutation had no effects on steady state activation (not shown) but significantly accelerated decay of the sodium current over a wide range of activation potentials (Fig. 9A–C). Steady state inactivation of A735V was unchanged compared to WT, displaying a $V_{1/2}$ of –68.5 ± 0.2 and –68.4 ± 0.1 mV, respectively. The R1192Q mutation produced a small but significant positive shift of steady state inactivation ($P < 0.05$) yielding a $V_{1/2}$ of –64.5 ± 0.2 mV. The protocol consisted of 500 ms conditioning pulses ranging from –140 to –60 mV in 5 mV increments followed by a test pulse to 10 mV. The holding potential was –90 mV.

Recovery from inactivation was significantly slower for A735V channels than for WT (Fig. 10), an effect similar to that

SUNDS A735V SCN5A MUTATION
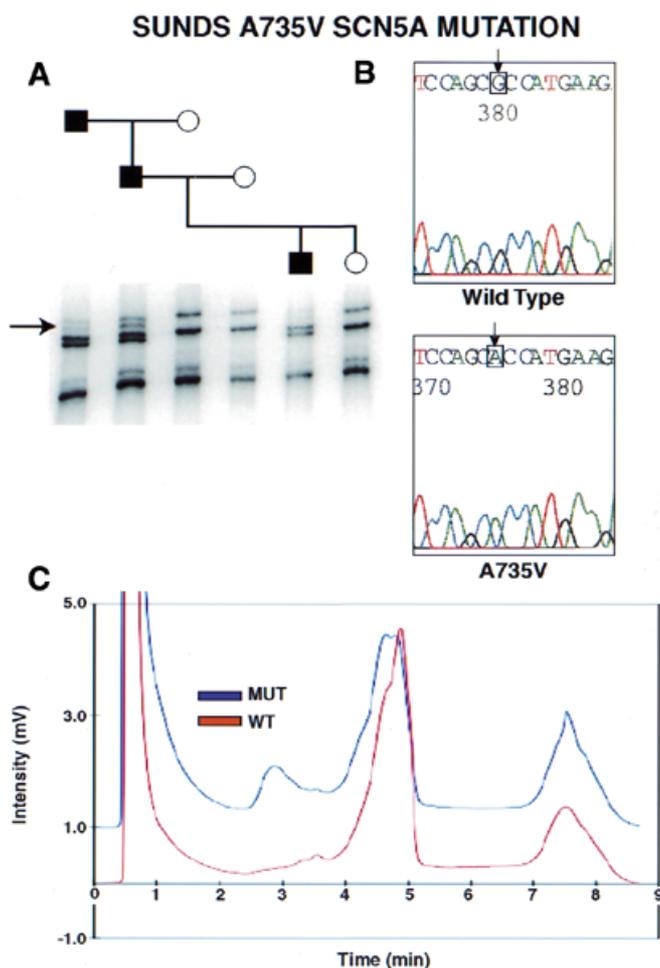
Figure 4. Mutation detection in Family M032. (**A**) SSCP analysis demonstrates an abnormal conformer (arrow) in affected individuals of this family in exon 14 of *SCN5A*. Note the pedigree which identifies three affected males. (**B**) DNA sequence analysis of the reverse primer product identifies a C→T substitution in exon 14 of *SCN5A* which results in substitution of the WT alanine by valine at codon 735 (A735V). (**C**) DHPLC confirms an abnormal band migration in affected individuals.

described previously for other Brugada syndrome-related mutations (9,10) but was not changed by the R1192Q mutation (data not shown).

DISCUSSION

Sudden cardiac death commonly results from ventricular arrhythmias, but the underlying mechanisms responsible for these tragic events are only now being unravelled. Over the past decade, two disorders in which ventricular arrhythmias play a central role in patient outcome, the long-QT (LQTS) and Brugada syndromes, have been characterized at the genetic level (16). In both instances, surface ECG abnormalities which could be explained by the genetic defects and resultant physiologic derangements, are notable. In LQTS, seven genetic loci have been identified (11–13,17) and the genes for six of these, all ion-channel-encoding genes, have been described (14). Five of these genes (*LQT1, LQT2, LQT5, LQT6* and *LQT7*) encode potassium channel proteins (*KVLQT1, minK, HERG, MiRP1*

and *Kir2.1*, respectively) whereas one, *LQT3*, encodes the cardiac sodium channel gene *SCN5A* (16). Similarly, Brugada syndrome has been shown to result from mutations in *SCN5A*, but the biophysical properties of mutant sodium channels differ in patients with LQTS (*LQT3*) (16,18,19) versus those with Brugada syndrome (9,10). Because SUNDS is characterized by ventricular tachyarrhythmias (VT/VF), has surface ECG abnormalities similar to those seen in Brugada syndrome, and is associated with nocturnal sudden death (1–4) like that described in some LQT3 patients (20), we screened patients and their families for *SCN5A* abnormalities. In two families with autosomal dominant inheritance, and one sporadic case, mutations were identified, all in the N-terminal portion of the SCN5A protein. Although we screened all families for mutations in the other ion channel candidate genes described above, no mutations other than in *SCN5A* were identified. In addition to LQTS, Brugada syndrome, and now SUNDS, mutations in *SCN5A* have also been found to cause progressive conduction system disease (Lev-Lenegre syndrome) (21), isolated conduction system disease (22), and sudden infant death syndrome (SIDS) (9,21,23,24). Interestingly, death most commonly occurs during sleep in all of these disorders, suggesting a common mechanism. Furthermore, mutations in *SCN5A* have been observed in patients with features of both LQTS and Brugada syndrome suggesting variable clinical presentations with mutations in the same gene (7,25). In family M033, the dizygotic twins presented during infancy, with one child dying of apparent SIDS, while his brother survived due to resuscitation of his ventricular tachyarrhythmias. Of note, previously reported Brugada mutations have been shown to cause the sodium channel to enter an intermediate inactivation state from which it recovers more slowly (26). Whereas this would lead to a reduction in I_{Na} at relatively rapid rates, it is not clear how this mechanism could contribute to the Brugada phenotype and arrhythmogenic substrate, both of which are bradycardia-dependent.

Biophysical analysis of the R367H mutation demonstrated non-functional channels with no expression of inward currents. To confirm that this was not due to a secondary mutation, the entire cDNA cassette was sequenced (data not shown) and the integrity of the RNA injected was assessed on a denaturing gel (data not shown). The A735V mutation resulted in the expression of robust I_{Na}, with steady state activation shifted towards more positive potentials, similar to that described previously for the Brugada syndrome at physiologic temperature (10). These channels displayed a slower recovery from inactivation than WT, again similar to that described previously for T1620M (9,10,27,28). The shift in A735V steady state activation leads to a shorter time to peak current as well as to reduced I_{Na} during a time and voltage corresponding to phase 1 of the right ventricular action potential. These two effects would be expected to reduce the contribution of I_{Na} during phase 1, leaving the transient outward current (I_{to}) unopposed.

The R1192Q mutation similarly shifts the balance of current towards I_{to} by accelerating the decay of I_{Na}. This effect is similar to that observed for two other Brugada mutations: T1620M (10) and L567Q (29,30).

Although different mechanisms are involved in A735V and R1192Q, the reduced density of I_{Na} present during activation of I_{to} (phases 0 and 1 of the action potential) can lead to an accentuation of the action potential notch and loss of the action
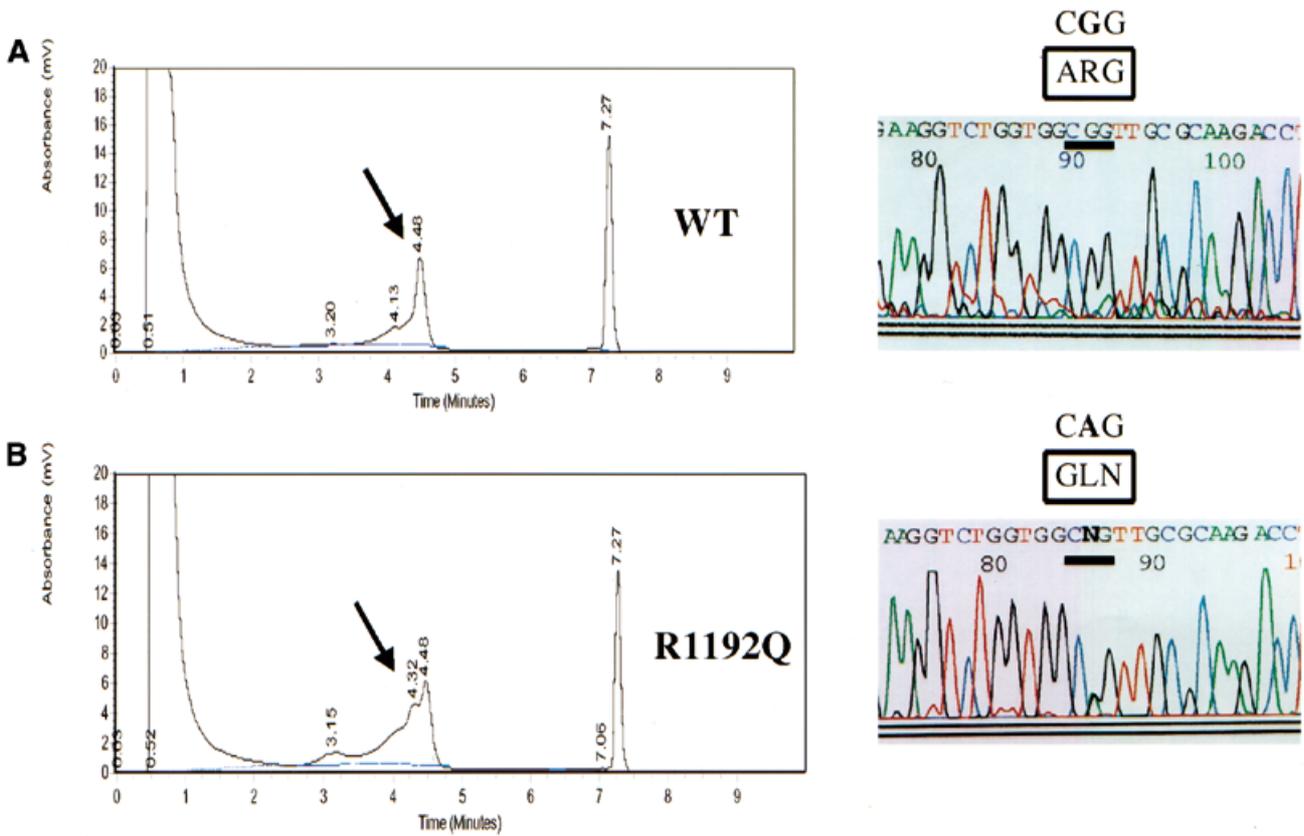
Figure 5. Mutation detection in family M033. (**A**) DHPLC identifies an abnormal band migration in exon 20 of SCN5A. (**B**) Sequence analysis demonstrates a G→A substitution nucleotide 3727, which results in substitution of arginine by glutamine at codon 1192 (R1192Q).
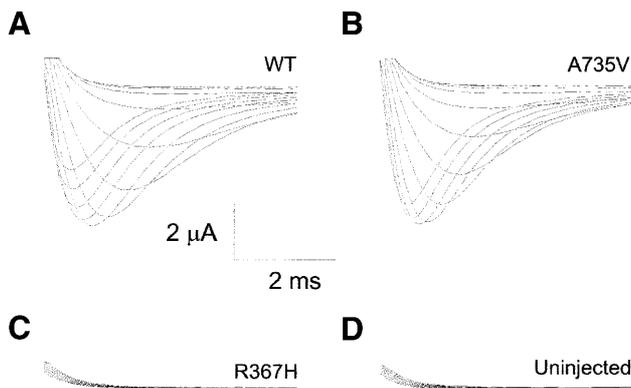
Figure 6. Heterologous expression of the A735V and R367H channels in *Xenopus laevis* oocytes. (**A**) WT *SCN5A*. (**B**) Mutant A735V. (**C**) Mutant R376H. (**D**) Endogenous currents. All currents were recorded using a 20 ms test pulse preceded by a 200 ms conditioning pulse to –120 mV from a holding potential of –90 mV. Current traces shown in (A–D) were elicited by potential steps from –40 to +10 mV in 5 mV increments.

potential dome. This rebalancing of net current present during phase 1 of the action potential can lead to loss of the action potential dome in cells possessing a prominent I_{to} (e.g. right ventricular epicardium) but not those largely devoid of an I_{to} (e.g. endocardium or left ventricular epicardium). Transmural or transepicardial dispersion is likely to develop as a consequence, leading to the ST-segment elevation in the right precordial leads (V1–V3) on surface ECG recordings and VT/VF, the hallmarks of both Brugada syndrome and SUNDS (31).

We conclude that Brugada syndrome and SUNDS represent the same autosomal dominant familial disorder, suggesting this disorder occurs worldwide. Both SUNDS and Brugada syndrome can result from mutations in the cardiac sodium channel SCN5A that cause loss of channel function but, like Brugada syndrome, mutations have only been identified in a proportion of the probands studied. Furthermore, this work suggests that SUNDS, Brugada syndrome, SIDS, LQTS and conduction system disease are allelic disorders, if not the same disease with variable penetrance and variable modifiers. The methods used to study these patients (PCR, SSCP and DHPLC), which are sensitive for the detection of point mutations or small deletions, could miss large gene deletions. Furthermore, promoter mutations resulting in aberrant gene expression cannot be discounted in patients testing negative for mutations. However, it appears likely that there is genetic heterogeneity in both of these disorders, with mutations in other ion channel genes or proteins involved in phase 1 repolarization of the ventricular action potential either directly or through modulation of ion channel function. Incomplete penetrance of these mutations could result in asymptomatic carriers. It is likely that provocation studies using ajmaline, flecainide or procainamide could be

A

B
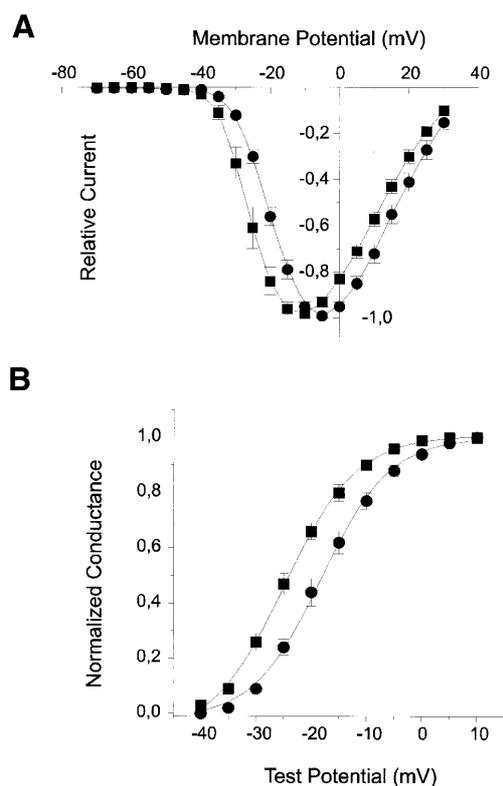
Figure 7. Steady state activation of the WT and A735V mutant channels. (**A**) Current–voltage relationship (*I–V*) of WT (squares, *n* = 6) and A735V (circles, *n* = 8) obtained from current recordings as illustrated in Figure 5. The peak current of A735V was significantly shifted from −10 to –5 mV when compared to WT. (**B**) Steady state activation was obtained by normalizing the chord conductance at each test potential of the *I–V* relationship to the maximal (slope) conductance. Data ± SEM were fitted to a Boltzmann distribution function (solid line) and yielded mid-activation potentials of −24.9 ± 0.4 mV (*n* = 8) and −18.2 ± 0.2 mV (*n* = 11) for WT and A735V, respectively.

useful in evaluation of asymptomatic SUNDS family members, as has been shown for Brugada syndrome (32,33). Finally, similar therapeutic options should be considered for both disorders; currently, implantation of an automatic implantable cardioverter defibrillator is an option to consider in these patients (2).

MATERIALS AND METHODS

Clinical evaluation

Kindreds and sporadic cases with clinical evidence of SUNDS were enrolled from medical clinics in Japan and Thailand. The phenotype of each family member was characterized by a previous history of sudden death in probands or in a family member, no demonstrable structural heart defects on echocardiogram or prolonged QT interval on surface ECG, and an ECG pattern of ST-segment elevation in leads V1–V3, with or without RBBB. Detailed family history was obtained from all probands and their families, along with the history of all clinical events. All enrolled individuals underwent evaluation by surface ECG and Holter monitor. When clinically indicated,

an electrophysiology study was performed. In all instances, written informed consent was obtained.

DNA mutation analysis

Genomic DNA was extracted directly from blood or from lymphoblastoid cell lines established from blood, using standard protocols (34). Genomic DNA samples were amplified by PCR using primers designed to amplify across the entire sequence of all known LQTS and Brugada syndrome genes (*KvLQT1, HERG, SCN5A, minK, MiRP1*) in an exon-by-exon manner (11–13). PCR products were analyzed by SSCP analysis (9,34) or by DHPLC using a WAVE DNA Fragment Analysis System (Transgenomic, Omaha, NE) (35). Normal and aberrant SSCP conformers were cut directly from dried gels and eluted in distilled water (65°C for 30 min) and then re-amplified. For samples giving abnormal DHPLC peaks, the genomic DNA was re-amplified directly. PCR products were sequenced, using Big Dye Terminator chemistry and an ABI-310 automated sequencer (PE Biosystems, Foster City, CA), according to the manufacturer's instructions. 100 control patients of Asian descent were used to exclude the likelihood of the abnormalities being benign polymorphisms.

Site-directed mutagenesis

Mutant *SCN5A* channel cDNAs were prepared by site-directed mutagenesis of the plasmid pcDNA–*SCN5A* which contains *SCN5A* cDNA cloned into pcDNA3.1+ (Invitrogen, Carlsbad, CA). To create the R367H mutant, the 'Megaprimer' method of mutagenesis was used. In brief, a 100 bp fragment containing the mutated sequence was amplified from pcDNA–*SCN5A* using the primers *SCN5A–Age*I (AGGGCTACCGGTGCCTAAAGGCAG) and *SCN5A–R367H* (CGTCATCAGGTGGAACACTG). After gel purification this was used as a 'megaprimer' along with *SCN5A–Nhe*I (CCGAGTCGTTCTTGCCAAAGAGCTG), to amplify a product of 1587 bp from pcDNA–*SCN5A*. This fragment was cloned back into pcDNA–*SCN5A* by substitution of the *Age*I–*Nhe*I fragment (nucleotides 1017–2536 of *SCN5A* cDNA).

A similar approach was used for constructing the A735V mutant. To create the 'megaprimer', pcDNA–*SCN5A* was amplified using the primers *SCN5A–A735V* (CACTCTTCAT-GGTGCTGGAG) and *SCN5A–Nhe*I. The 408 bp PCR megaprimer was then used with *SCN5A–Age*I to amplify the 1587 bp product, which was cloned in pcDNA–*SCN5A* as above. Mutant clones were identified and characterized by DNA sequencing with *SCN5A–Age*I or *SCN5A–Nhe*I primers, as described above.

Oocyte preparation, RNA injection and electrophysiology

Xenopus laevis were anesthetized and an incision was made in the lower abdomen of the frogs to remove the ovarian lobes. The oocytes were freed from the lobes and digested for 1–2 h with 2 mg/ml collagenase (201 U/mg; Gibco BRL, Gaithersburg, MD) to remove the follicular membrane. Healthy stage IV and V oocytes were selected for RNA injection on the next day.

In vitro transcription of WT and mutant *SCN5A* cDNAs was performed using an mMessage mMachine kit (Ambion, Austin, TX). The RNA solution was diluted to the desired concentration (250 or 500 ng/µl) in sterile 100 mM KCl and
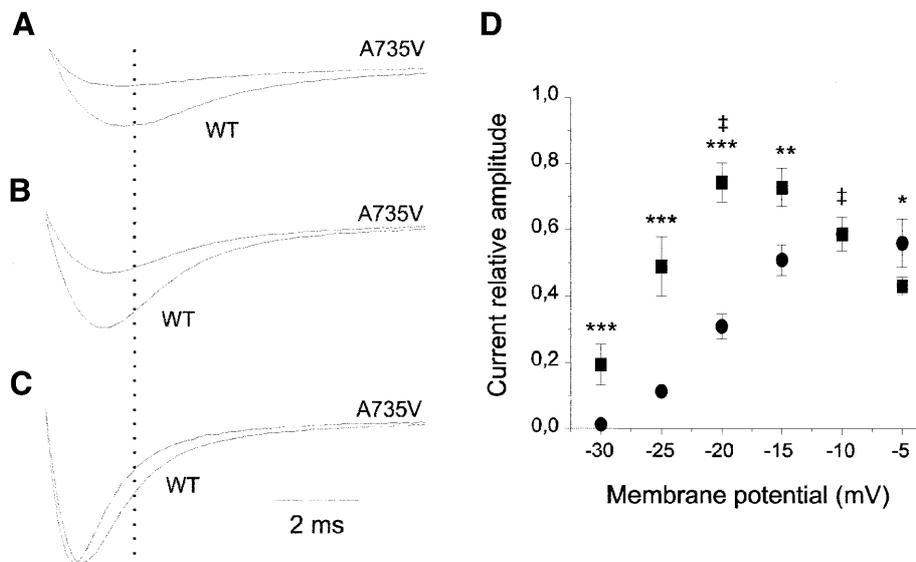
Figure 8. Effects of the steady state activation shift on the current decay of A735V in a range of potentials corresponding to the end of phase 1 of the action potential. (**A**) Current traces from WT and A735V during a test pulse to –30 mV were normalized to their respective maximal currents and superimposed. Although the two current traces have the same time constants for decay kinetics, the contribution of A735V is significantly reduced over a time course of 4 ms when compared to WT due to the 7 mV shift in steady state activation between the two channels (Fig. 6). (**B**) Current traces, as described in (A), obtained at −25 mV. (**C**) Maximal peak currents of representative WT and A735V recordings are superimposed (WT, −15 mV; A735V, –5 mV). (**D**) Relative current values as described in (A−C) were measured 3 ms after the start of the test pulse (dotted line) and plotted as a function of the test potential for WT (squares) and A735V (circles). ***$P < 0.001$, *$P < 0.05$ for values at the same potential, ‡$P < 0.05$ between the marked values, each corresponding to the location of the maximal peak current as shown in (C).
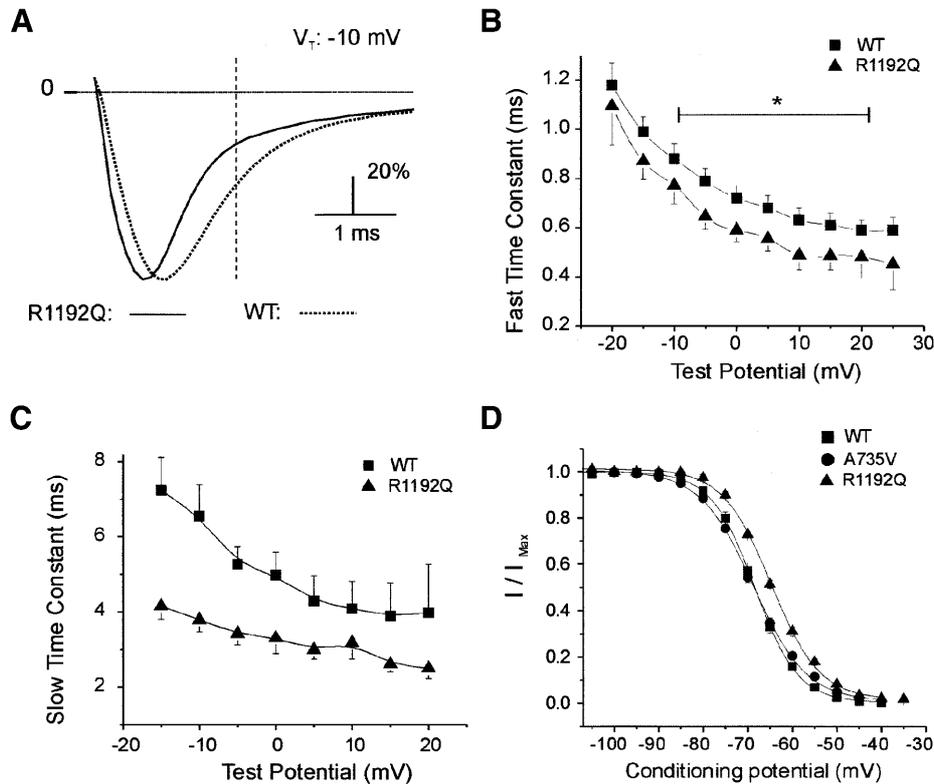
Figure 9. R1192Q mutation accelerates fast inactivation of the sodium channel. (**A**) Representative currents recorded from WT (dotted line) and mutated channels (R1192Q, solid line) following a pulse to –10 mV from a holding potential of –120 mV. Currents were normalized to their respective peak values (R1192Q, 4.7 μA; WT, 5.6 μA). The dashed line 3 ms after the beginning of the pulse indicates the timing of peak transient outward current. 0 indicates the baseline level. (**B** and **C**) Current decay was fitted to a sum of two exponentials and the fast and slow time constants of each parameter were plotted against the membrane potential. In (B), values were statistically significant only in the range specified by the line labeled with an asterisk ($P < 0.05$). In (C), all values were statistically different ($P < 0.01$ except at −10 mV). Number of cells tested: WT, 8; R1192Q, 12. (**D**) The R1192Q mutation significantly shifted the steady state mid-inactivation potential by +5 mV but A735V had no effect on the availability of the channels. Data ± SEM were fitted to a standard Boltzmann distribution function (solid line). Number of cells tested: WT, 11; A735V, 8; R1192Q, 18.
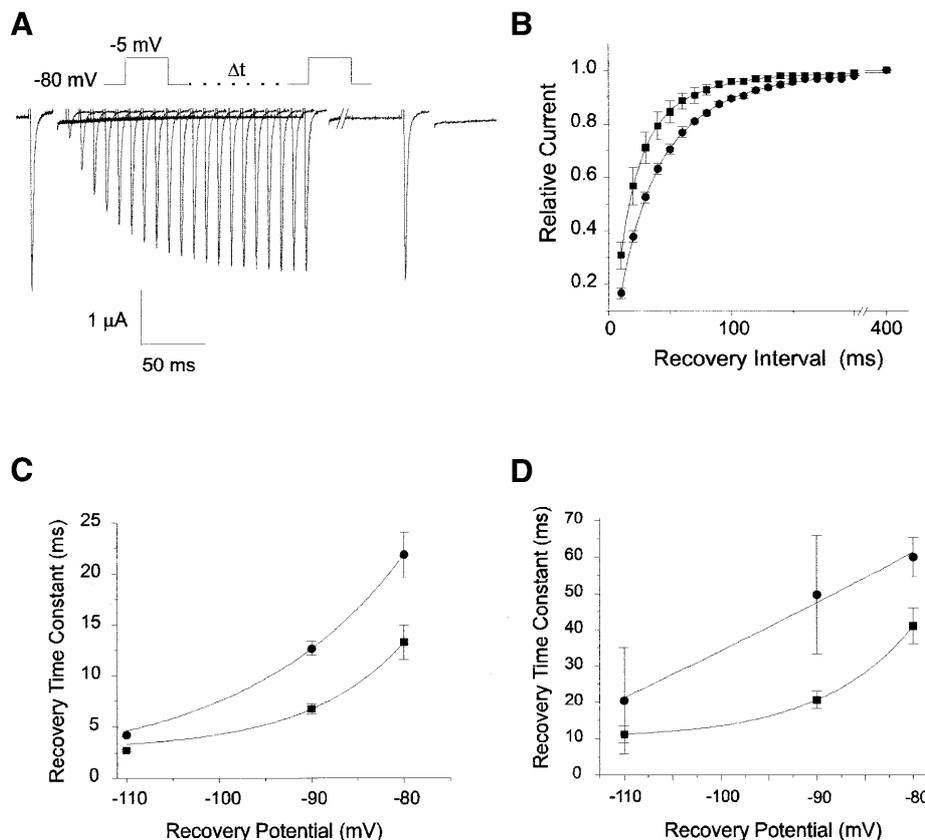
Figure 10. Recovery from inactivation of WT and A735V mutant channels. (**A**) Recovery from inactivation was measured using a standard double pulse protocol with varying recovery inter-pulse interval (Δt) duration as shown for the WT currents. (**B**) Peak current elicited during the second pulse was normalized to the value obtained during the initial test pulse. The ratio was then plotted as a function of the recovery potential during the inter-pulse. Data ± SEM for WT (squares) and A735V (circles) were fitted to a sum of two exponential functions (solid line) with values of 59 ± 5 (41%) and 21 ± 2 ms (59%), and 40 ± 5 (31%) and 13 ± 2 (69%) ms for the slow and fast recovery components of WT and A735V currents, respectively. Fast (**C**) and slow (**D**) components of recovery were slower for A735V at all recovery potentials studied.

46 nl of the cRNA solution was injected in each oocyte using a Nanojet automatic oocyte injector (Drummond Instruments, Broomall, PA). Once injected, the eggs were stored at 17°C in SOS solution containing 100 mM NaCl, 2 mM KCl, 1.8 mM $CaCl_2 \cdot 2H_2O$, 1 mM $MgCl_2 \cdot 6H_2O$, 5 mM HEPES, 2.5 mM pyruvic acid, pH 7.6, supplemented with 100 μg gentamicin, 100 U/ml penicillin + 100 μg/ml streptomycin, under slow shaking.

Whole-cell currents were recorded from *Xenopus* oocytes using the conventional two-microelectrode voltage-clamp technique (10). Briefly, bevelled microelectrodes were plugged with a 1.5% agarose solution containing 3 M KCl, 10 mM HEPES and 10 mM EGTA, pH 7.4 and back-filled with 3 M KCl to give a resistance of 0.2–0.5 MΩ. Oocytes were placed in a chamber and perfused with an external solution containing 5 mM KCl, 2 mM $CaCl_2$, 1 mM $MgCl_2$, 140 mM NaOH, 10 mM HEPES, 10 mM glucose, pH 7.4. Currents were amplified by a Warner oocytes clamp (OC-725A), low-pass filtered at 3 kHz (−3 dB, 4 pole Bessel filter, Wavetech, Model 432). Data acquisition and analysis was performed with pCLAMP 6 (Axon Instruments, Foster City, CA). Currents were recorded at room temperature, and experiments in which the holding current was >200 nA at a holding potential of −90 mV were excluded from analysis.

REFERENCES

1. Baron,R.C., Thacker,S.B., Gorelkin,L., Vernon,A.A., Taylor,W.R. and Choi,K. (1983) Sudden death among Southeast Asian refugees. An unexplained nocturnal phenomenon. *J. Am. Med. Assoc.*, **250**, 2947–2951.
2. Nademanee,K., Veerakul,G., Nimmannit,S., Chaowakul,V., Bhuripanyo,K., Likittanasombat,K., Tunsanga,K., Kuasirikul,S., Malasit,P., Tansupasawadikul,S. *et al.* (1997) Arrhythmogenic marker for the sudden unexplained death syndrome in Thai men. *Circulation*, **96**, 2595–2600.

3. Gilbert,J., Gold,R.L., Haffajee,C.I. and Alpert,J.S. (1986) Sudden cardiac death in a southeast Asian immigrant: clinical, electrophysiologic and biopsy characteristics. *Pacing Clin. Electrophysiol.*, **9**, 912–914.

4. Brugada,P. and Brugada,J. (1992) Right bundle branch block, persistent ST segment elevation and sudden cardiac death: a distinct clinical and electrocardiographic syndrome. A multicenter report. *J. Am. Coll. Cardiol.*, **20**, 1391–1396.

5. Brugada,J. and Brugada,P. (1997) Further characterization of the syndrome of right bundle branch block, ST segment elevation and sudden cardiac death. *J. Cardiovasc. Electrophysiol.*, **8**, 325–331.

6. Kobayashi,T., Shintani,U., Yamamoto,T., Shida,S., Isshiki,N., Tanaka,T., Ohmoto,Y., Kitamura,M., Kato,S. and Misaki,M. (1996) Familial occurrence of electrocardiographic abnormalities of the Brugada-type. *Intern. Med.*, **35**, 637–640.

7. Bezzina,C., Veldkamp,M.W., van Den Berg,M.P., Postma,A.V., Rook,M.B., Viersma,J.W., van Langen,I.M., Tan-Sindhunata,G., Bink-Boelkens,M.T., van Der Hout,A.H. *et al.* (1999) A single Na(+) channel mutation causing both long-QT and Brugada syndromes. *Circ. Res.*, **85**, 1206–1213.

8. Rook,M.B., Alshinawi,C.B., Groenewegen,W.A., van Gelder,I.C., van Ginneken,A.C., Jongsma,H.J., Mannens,M.M. and Wilde,A.A. (1999) Human SCN5A gene mutations alter cardiac sodium channel kinetics and are associated with the Brugada syndrome. *Cardiovasc. Res.*, **44**, 507–517.

9. Chen,Q., Kirsch,G.E., Zhang,D., Brugada,R., Brugada,J., Brugada,P., Potenza,D., Moya,A., Borggrefe,M., Breithardt,G. *et al.* (1998) Genetic basis and molecular mechanism for idiopathic ventricular fibrillation. *Nature*, **392**, 293–296.

10. Dumaine,R., Towbin,J.A., Brugada,P., Vatta,M., Nesterenko,D.V., Nesterenko,V.V., Brugada,J., Brugada,R. and Antzelevitch,C. (1999) Ionic mechanisms responsible for the electrocardiographic phenotype of the Brugada syndrome are temperature dependent. *Circ. Res.*, **85**, 803–809.

11. Splawski,I., Shen,J., Timothy,K.W., Vincent,G.M., Lehmann,M.H. and Keating,M.T. (1998) Genomic structure of three long QT syndrome genes: KVLQT1, HERG and KCNE1. *Genomics*, **51**, 86–97.

12. Schulze-Bahr,E., Wang,Q., Wedekind,H., Haverkamp,W., Chen,Q., Sun,Y., Rubie,C., Hordt,M., Towbin,J.A., Borggrefe,M. *et al.* (1997) KCNE1 mutations cause Jervell and Lange-Nielsen syndrome. *Nat. Genet.*, **17**, 267–268.

13. Abbott,G.W., Sesti,F., Splawski,I., Buck,M.E., Lehmann,M.H., Timothy,K.W., Keating,M.T. and Goldstein,S.A. (1999) MiRP1 forms IKr potassium channels with HERG and is associated with cardiac arrhythmia. *Cell*, **97**, 175–187.

14. Suzuki, H., Torigoe, K, Numata, O. and Yazaki, S. (2000) Infant case with a malignant form of Brugada syndrome. *J. Cardiovasc. Electrophysiol.*, **11**, 1277–1280.

15. Marban,E., Yamagishi,T. and Tomaselli,G.F. (1998) Structure and function of voltage-gated sodium channels. *J. Physiol. (Lond.)*, **508**, 647–657.

16. Vatta,M., Li,H. and Towbin,J.A. (2000) Molecular biology of arrhythmic syndromes. *Curr. Opin. Cardiol.*, **15**, 12–22.

17. Plaster,N.M., Tawil,R., Tristani-Firouzi,M., Canun,S., Bendahhou,S., Tsunoda,A., Donaldson,M.R., Iannaccone,S.T., Brunt,E., Barohn,R. *et al.* (2001) Mutations in Kir2.1 cause the developmental and episodic electrical phenotypes of Andersen's syndrome. *Cell*, **105**, 511–519.

18. Dumaine,R., Wang,Q., Keating,M.T., Hartmann,H.A., Schwartz,P.J., Brown,A.M. and Kirsch,G.E. (1996) Multiple mechanisms of Na$^+$ channel-linked long-QT syndrome. *Circ. Res.*, **78**, 916–924.

19. Bennett,P.B., Yazawa,K., Makita,N. and George,A.L.,Jr (1995) Molecular mechanism for an inherited cardiac arrhythmia. *Nature*, **376**, 683–685.

20. Zareba,W., Moss,A.J., Schwartz,P.J., Vincent,G.M., Robinson,J.L., Priori,S.G., Benhorin,J., Locati,E.H., Towbin,J.A., Keating,M.T. *et al.* (1998) Influence of genotype on the clinical course of the long-QT syndrome. International Long-QT Syndrome Registry Research Group. *New Engl. J. Med.*, **339**, 960–965.

21. Schott,J.J., Alshinawi,C., Kyndt,F., Probst,V., Hoorntje,T.M., Hulsbeek,M., Wilde,A.A., Escande,D., Mannens,M.M. and Le Marec,H. (1999) Cardiac conduction defects associate with mutations in SCN5A. *Nat. Genet.*, **23**, 20–21.

22. Tan,H.L., Bink-Boelkens,M.T., Bezzina,C.R., Viswanathan,P.C., Beaufort-Krol,G.C., van Tintelen,P.J., van den Berg,M.P., Wilde,A.A. and Balser,J.R. (2001) A sodium-channel mutation causes isolated cardiac conduction disease. *Nature*, **409**, 1043–1047.

23. Splawski,I., Shen,J., Timothy,K.W., Lehmann,M.H., Priori,S., Robinson,J.L., Moss,A.J., Schwartz,P.J., Towbin,J.A., Vincent,G.M. *et al.* (2000) Spectrum of mutations in long-QT syndrome genes. KVLQT1, HERG, SCN5A, KCNE1 and KCNE2. *Circulation*, **102**, 1178–1185.

24. Schwartz,P.J., Priori,S.G., Dumaine,R., Napolitano,C., Antzelevitch,C., Stramba-Badiale,M., Richard,T.A., Berti,M.R. and Bloise,R. (2000) A molecular link between the sudden infant death syndrome and the long-QT syndrome. *New Engl. J. Med.*, **343**, 262–267.

25. Deschenes,I., Baroudi,G., Berthet,M., Barde,I., Chalvidan,T., Denjoy,I., Guicheney,P. and Chahine,M. (2000) Electrophysiological characterization of SCN5A mutations causing long QT (E1784K) and Brugada (R1512W and R1432G) syndromes. *Cardiovasc. Res.*, **46**, 55–65.

26. Wang,D.W., Makita,N., Kitabatake,A., Balser,J.R. and George,A.L.,Jr (2000) Enhanced Na(+) channel intermediate inactivation in Brugada syndrome. *Circ. Res.*, **87**, E37–E43.

27. Baroudi,G., Carbonneau,E., Pouliot,V. and Chahine,M. (2000) SCN5A mutation (T1620M) causing Brugada syndrome exhibits different phenotypes when expressed in *Xenopus* oocytes and mammalian cells. *FEBS Lett.*, **467**, 12–16.

28. Makita,N., Shirai,N., Wang,D.W., Sasaki,K., George,A.L.,Jr, Kanno,M. and Kitabatake,A. (2000) Cardiac Na(+) channel dysfunction in Brugada syndrome is aggravated by β(1)-subunit. *Circulation*, **101**, 54–60.

29. Antzelevitch,C. (2001) Molecular biology and cellular mechanisms of cardiac arrhythmias and sudden death in infants and young children. *J. Electrocardiol.*, **34**, 320.

30. Wan,X., Chen,S., Sadeghpour,A., Wang,Q. and Kirsch,G.E. (2001) Accelerated inactivation in a mutant Na(+) channel associated with idiopathic ventricular fibrillation. *Am. J. Physiol. Heart Circ. Physiol.*, **280**, H354–H360.

31. Yan,G.X. and Antzelevitch,C. (1999) Cellular basis for the Brugada syndrome and other mechanisms of arrhythmogenesis associated with ST-segment elevation. *Circulation*, **100**, 1660–1666.

32. Antzelevitch,C., Brugada,P., Brugada,J., Brugada,R., Nademanee,K. and Towbin,J. (1999) The Brugada syndrome. In Camm,A.J. (ed.), *Clinical Approaches to Tachyarrhythmias*. Futura Publishing Co., Armonk, NY.

33. Brugada,R., Brugada,J., Antzelevitch,C., Kirsch,G.E., Potenza,D., Towbin,J.A. and Brugada,P. (2000) Sodium channel blockers identify risk for sudden death in patients with ST-segment elevation and right bundle branch block but structurally normal hearts. *Circulation*, **101**, 510–515.

34. Li,H., Chen,Q., Moss,A.J., Robinson,J., Goytia,V., Perry,J.C., Vincent,G.M., Priori,S.G., Lehmann,M.H., Denfield,S.W. *et al.* (1998) New mutations in the KVLQT1 potassium channel that cause long-QT syndrome. *Circulation*, **97**, 1264–1269.

35. Bowles,K.R., Abraham,S.E., Brugada,R., Zintz,C., Comeaux,J., Sorajja,D., Tsubata,S., Li,H., Brandon,L., Gibbs,R.A. *et al.* (2000) Construction of a high-resolution physical map of the chromosome 10q22–q23 dilated cardiomyopathy locus and analysis of candidate genes. *Genomics*, **67**, 109–127.